

Alcohol-Based Digital Etch for III–V Vertical Nanowires With Sub-10 nm Diameter

Wenjie Lu, *Student Member, IEEE*, Xin Zhao, *Student Member, IEEE*, Dongsung Choi, Salim El Kazzi, and Jesús A. del Alamo, *Fellow, IEEE*

Abstract—This letter introduces a novel alcohol-based digital etch technique for III–V FinFET and nanowire MOSFET fabrication. The new technique addresses the limitations of the conventional water-based approach in enabling structures with sub-10-nm 3-D features. Using the same oxidation step, the new technique shows an etch rate of 1 nm/cycle, identical to the conventional approach. Sub-10 nm fins and nanowires with a high mechanical yield have been achieved. InGaAs nanowires with a diameter of 5 nm and an aspect ratio greater than 40 have been demonstrated. The new technique has also been successfully applied to InGaSb-based heterostructures, the first demonstration of digital etch in this material system. Vertical InGaAs nanowire gate-all-around MOSFETs with a sub-threshold swing of 70 mV/decade at $V_{DS} = 50$ mV have been obtained at a nanowire diameter of 40 nm, demonstrating the good interfacial quality that the new technique provides.

Index Terms—Digital etch, InGaAs, InGaSb, nanowire, FinFETs, nanowire MOSFETs.

I. INTRODUCTION

III–V COMPOUND semiconductors are regarded as promising candidates to replace silicon in future generations of CMOS technology. In the quest for enhanced performance over silicon devices at advanced nodes, III–V multi-gate transistors such as FinFETs or nanowire gate-all-around MOSFETs (NW-MOSFETs) are being pursued with fin width or nanowire diameter in the sub-10 nm range. In this dimensional regime, precise etching control is paramount.

Inspired by the atomic layer etching technology developed in silicon [1], [2], the concept of digital etch (DE) was introduced to III–V compound semiconductors [3]–[8]. In digital etch, the oxidation and oxide removal steps characteristic of chemical etching are performed separately. This makes them both self-limiting affording nanometer-scale control of the etching process. Digital etch has been shown to preserve high aspect ratio features, enabling precise device dimension

Manuscript received March 3, 2017; revised March 26, 2017; accepted March 27, 2017. Date of publication April 3, 2017; date of current version April 24, 2017. This work was supported in part by Samsung Electronics, in part by Defense Threat Reduction Agency under Grant HDTRA 1-14-1-0057, in part by the NSF Center for Energy Efficient Electronics Science under Award 0939514, in part by Lam Research, and in part by the Korea Institute of Science and Technology. The review of this letter was arranged by Editor D.-H. Kim. (*Corresponding author: Wenjie Lu.*)

W. Lu, X. Zhao, D. Choi, and J. A. del Alamo are with the Microsystems Technology Laboratories, Massachusetts Institute of Technology, Cambridge, MA 02139 USA (e-mail: wenjie@mit.edu).

S. El Kazzi is with imec, 3001 Leuven, Belgium.

Color versions of one or more of the figures in this letter are available online at <http://ieeexplore.ieee.org>.

Digital Object Identifier 10.1109/LED.2017.2690598

engineering. It has also been shown to be effective in mitigating surface damage induced by RIE [9]. In the last few years, the use of digital etch has enabled demonstrations of aggressively scaled III–V FinFETs and NW-MOSFETs with exciting electrical characteristics [10]–[14].

So far, DE has been solely applied to arsenide-based III–Vs, achieving a smallest feature size of 5 nm in fins [15] and 7 nm in lateral nanowires [10]. On the other hand, demonstrations of high aspect ratio vertical nanowires (VNW) by DE have been limited to 11–15 nm diameter [12]. This is a result of nanowire breakage as a consequence of the strong mechanical stress exerted by the water-based acids used in the oxide removal step of DE. In addition, conventional DE does not work on antimonide-based III–Vs, an important class of materials with potential for p-channel MOSFETs and tunnel-FETs [12], [16]–[18]. Antimonides are highly reactive and can be etched by water, negating the tight etching control that is sought in DE.

In this letter, we introduce a novel non-aqueous DE technique that overcomes these challenges. The new approach uses acids dissolved in alcohol which has less surface tension than water. We obtain a consistent 1 nm/cycle etching rate on both InGaAs and InGaSb-based heterostructures. We also demonstrate a 97% mechanical yield of sub-10 nm VNWs after 7 etch cycles. In addition, we show InGaAs vertical single NW-MOSFETs fabricated by this technique with excellent subthreshold characteristics.

II. EXPERIMENT

DE of a III–V semiconductor consists of an oxidation step, typically performed dry in oxygen plasma [7], or wet in ozonated water [13] or H_2O_2 [3], [4], followed by an oxide removal step, conventionally carried in water-based H_2SO_4 [3], [9], [11] or HCl [3], [10], [12], [13]. When performed separately, both steps are self-limiting resulting in a highly controlled etch rate in the nanometer per cycle range.

We explore the use of alcohol-based acids for the oxide removal sub-cycle. The motivation is twofold. On the one hand, we seek to reduce the surface tension of the acid removal step in an effort to enhance the survivability of very thin nanowires. Secondly, we seek a DE technique for antimonides which are highly reactive and easily oxidized and etched in water. This is particularly the case if there are defects from material growth or plasma damage.

We compare three oxide removal chemistries: 4.1 M H_2SO_4 in DI water, 2.0 M H_2SO_4 in methanol, and 0.1 M HCl in isopropanol IPA.¹ H_2SO_4 and HCl are chosen as they are

¹The solvent-based acids are commercially available at Sigma-Aldrich Co., as methanolic H_2SO_4 and HCl-2-propanol solution.

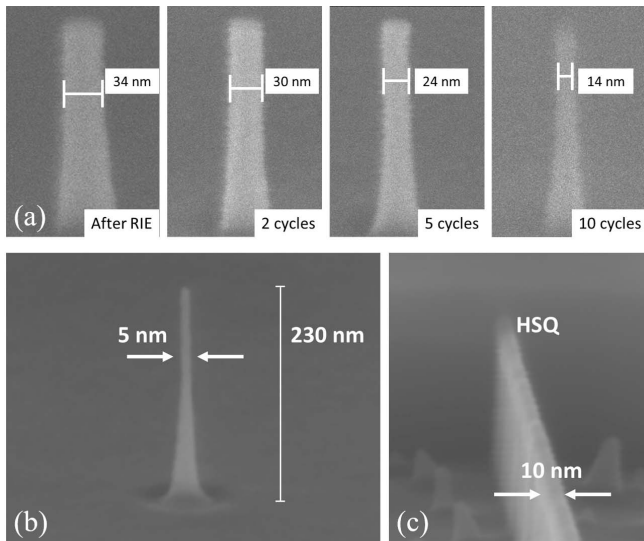


Fig. 1. (a) Evolution of InGaAs VNWs in a sequential etch experiment involving different numbers of digital etch cycles in 10% HCl:IPA. (b) InGaAs VNW with 5 nm diameter, 230 nm height obtained after 10 cycles of digital etch in H_2SO_4 :methanol. (c) 10 nm wide InGaSb fin obtained after 5 cycles of digital etching in HCl:IPA.

the most used acids for InGaAs DE. For antimonides, only HCl-based etch is studied since antimonides are attacked by H_2SO_4 . In all cases, oxidation is performed in oxygen plasma for 3 min in a barrel asher. The starting arsenide heterostructure consists of multiple layers of $\text{In}_{0.53}\text{Ga}_{0.47}\text{As}$ and $\text{In}_{0.52}\text{Al}_{0.48}\text{As}$ grown by MBE on an InP substrate. The antimonide heterostructure consists of 20 nm of $\text{In}_{0.28}\text{Ga}_{0.62}\text{Sb}$ on 200 nm $\text{Al}_{0.65}\text{Ga}_{0.35}\text{Sb}$ buffer, grown by MBE on a GaAs substrate. After standard surface cleaning and native oxide removal, a 2 nm Si_3N_4 adhesion layer is deposited, followed by 100 nm hydrogen silsesquioxane (HSQ). Fin and vertical nanowire patterns are defined by e-beam lithography. The samples are then dry etched by $\text{BCl}_3/\text{Ar}/\text{SiCl}_4$ ICP at 250 °C for 2 min [9], resulting in a final fin or VNW height of about 230 nm.

After RIE, the arsenide sample is dipped in BOE for 30 s to remove the HSQ mask and native oxide. The antimonide sample is dipped in the HCl:IPA solution for 30 s, to remove the native oxide, with the HSQ remaining. At this point, various cycles of digital etch are carried out. Between cycles, fin width and VNW diameter are measured by SEM to monitor the etch rate. Fig. 1(a) demonstrates the thinning process of an arsenide VNW with initial diameter of 34 nm, after 2, 5, and 10 DE cycles in HCl:IPA. Fig. 1(b) shows the narrowest arsenide VNW obtained with a 5 nm diameter and 230 nm height (aspect ratio = 46). Fig. 1(c) shows a 10 nm wide antimonide fin.

III. RESULTS AND DISCUSSION

Etch-rates were obtained by measuring VNW diameter by SEM on sets of 12 NWs of various initial diameters. Figs. 2(a) and (b) show the evolution of arsenide NW diameter in alcohol-based HCl and H_2SO_4 , respectively. The average radial etch rate in HCl:IPA is 1.0 ± 0.04 nm/cycle, and in H_2SO_4 :methanol is 1.2 ± 0.05 nm/cycle. These values closely match the etch rate using H_2SO_4 :DI water which is 1.0 ± 0.1 nm/cycle.

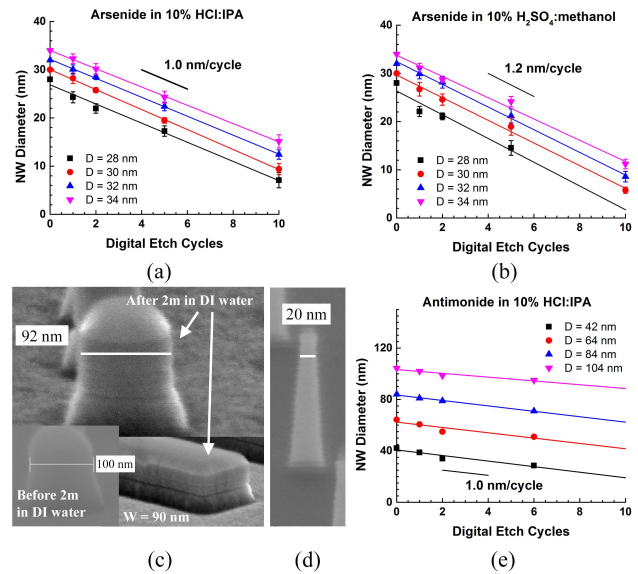


Fig. 2. Evolution of arsenide VNW diameter with number of DE cycles in (a) 10% HCl:IPA; (b) 10% H_2SO_4 :methanol; (c) Antimonide VNW and fin before and after dipping in DI water for 2 min; (d) Antimonide VNW after dipping in HCl:IPA for 2 min; (e) Same as (a) but for antimonide VNW in 10% HCl:IPA. In (a), (b) and (e) the legends indicate the initial VNW diameter after RIE.

Fig. 2(c) shows the change in an antimonide NW after dipping in DI water for 2 minutes. The diameter decreases from 100 nm to 92 nm. Also, the NW sidewall and AlGaSb field surface become rough and trenches appear at the hetero-junction interfaces. The antimonide fin sidewall in Fig. 2(c) also reveals such etching. Therefore, water-based DE is not viable for antimonides. This issue is relieved by using alcohol-based solutions. Fig. 2(d) shows an antimonide NW after dipping in 10% HCl:IPA for 2 minutes. No excessive sidewall etching or surface damage is observed, implying that the etching is self-limited after removing the layer of oxide on the sidewall. Fig. 2(e) shows the HCl:IPA digital etch rate of antimonide NWs, exhibiting a radial etching rate of 1.0 ± 0.1 nm/cycle.

A key challenge for devices fabricated by DE is the low mechanical yield of the process in the sub-10 nm regime. This is a result of the high surface tension of water during dipping and rinsing, and is particularly problematic for VNWs which, unlike fins, cannot be anchored at both ends. Fig. 3(a) shows an arsenide VNW array (initial diameter = 22 nm) after 7 cycles of conventional DE. A final NW diameter of 8 nm is expected but all structures are destroyed. In contrast, Fig. 3(b) shows an identical sample processed side-by-side in HCl:IPA. 8 nm diameter VNWs are demonstrated with over 97% mechanical yield. Moreover, no clustering is observed for tightly spaced VNWs [19]. This is revealed in Fig. 3(d) where a 10 nm diameter VNW array spaced by 80 nm is shown.

Table 1 summarizes the mechanical yield of arsenide VNWs after 7 DE cycles with various nominal final diameters, for water as well as alcohol-based acids. The superiority of the new technique is clearly demonstrated. It should be noted that 7 DE cycles is a harsh process that is typically unnecessary in actual device fabrication. In a shortened process, higher mechanical yields at smaller diameters should be possible.

It is worth noting that, although there are other drying methods which can minimize surface tension, such as critical

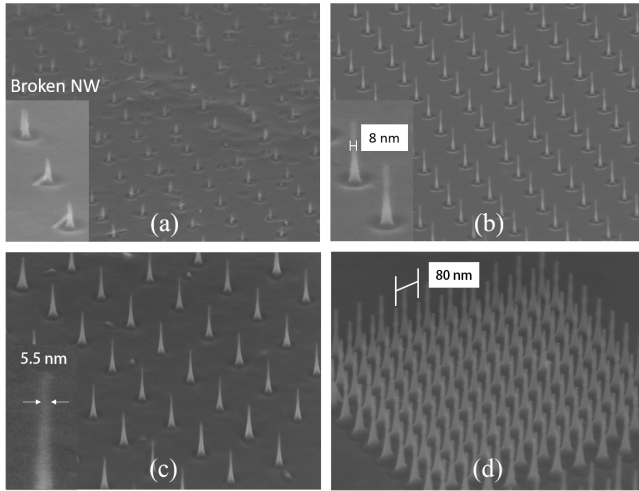


Fig. 3. Arsenide VNW array after 7 DE cycles in (a) 10% HCl in DI water, (b) 10% HCl in IPA, and (c) 10% H_2SO_4 in methanol. The insets show close ups of the etched structures. The nanowire mechanical yield in (a) is 0%, while the one in (b) is 97% and in (c) is 90%. (d) Tightly-packed arsenide VNW array after 7 DE cycles in 10% HCl:IPA. The NW diameter is 10 nm and spacing is 80 nm.

TABLE I
MECHANICAL YIELD OF InGaAs VNWs AFTER 7 CYCLES
OF DIGITAL ETCH

D_{Initial} (nm)	D_{Final} (nm)	DE:HCl/H ₂ O Rinse:H ₂ O	DE:HCl/IPA Rinse:IPA	DE:H ₂ SO ₄ /methanol Rinse:IPA	DE:HCl/H ₂ O Rinse:IPA
28	14	100%	100%	100%	100%
26	12	31%	100%	100%	100%
24	10	5%	100%	100%	0%
22	8	0%	97%	95%	0%
20	6	0%	5%	90%	0%

point drying (CPD), a solvent-based treatment is most compatible with CMOS manufacturing. Drying methods such as CPD are often time consuming, making them infeasible when multiple cycles of DE are required. In addition, breakage of VNWs can happen both in the etching and rinsing steps. To clarify the relative contributions, Table 1 includes the mechanical yield of methanolic H_2SO_4 DE, and aqueous HCl DE with IPA rinsing. Although IPA rinsing improves the mechanical yield of HCl:H₂O DE drastically at $D = 12$ nm, it shows no difference at and below 10 nm. Interestingly, the H_2SO_4 :methanol DE shows much better yield at the smallest final diameter of 6 nm than the HCl:IPA DE, even though both methods are rinsed with IPA. This is shown in Fig. 3(c). This is likely due to the smaller viscosity of methanol (0.54 cP) than that of IPA (2.0 cP). These results indicate that NW breakage happens during the oxide etch process as well as while rinsing.

IV. InGaAs NW-MOSFETs

To illustrate the practical applicability of the new DE process, we have fabricated InGaAs VNW-MOSFETs through a process similar to that of [14] using a similar heterostructure to [20]. The process includes 5 DE cycles in 4.1 M H_2SO_4 :methanol. Fig. 4(a) shows a schematic cross-section of the device which features a 2 nm thick Al_2O_3 gate dielectric (EOT = 1 nm), W gate metal, and Mo ohmic contacts.

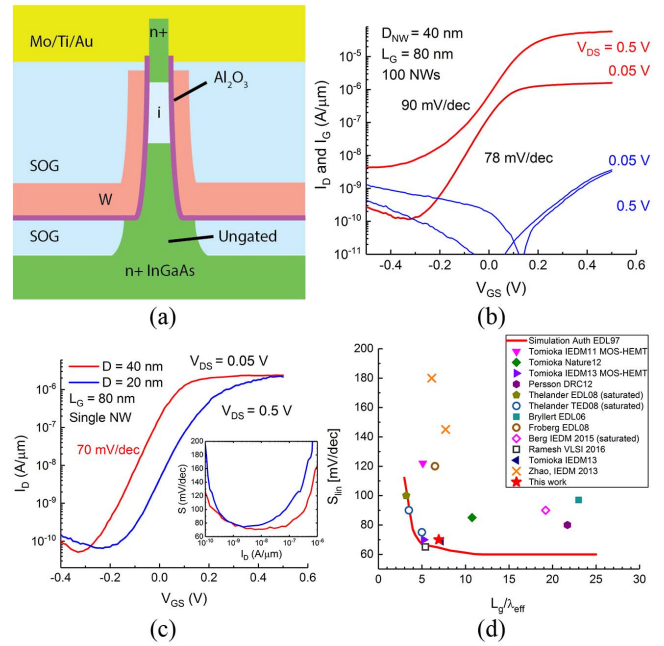


Fig. 4. (a) Schematic cross-section of InGaAs VNW-MOSFET; (b) subthreshold characteristics for a VNW transistor array with $D = 40$ nm and 100 VNWs, treated with 5 DE cycles in H_2SO_4 :methanol; (c) subthreshold characteristics of a single VNW transistor with $D = 40$ nm with lowest S_{lin} of 70 mV/dec. The inset shows S vs. I_D of this device. (d) Linear subthreshold swing vs. ratio of gate length to natural length of InGaAs VNW MOSFETs.

NW diameters range from 20 to 40 nm, the channel length is 80 nm.

The linear subthreshold characteristics of a typical device consisting of 100 NWs with 40 nm diameter is shown in Fig. 4(b). A linear subthreshold swing, S_{lin} , of 78 mV/dec is obtained on the NW array. As shown in Fig. 4(c), a single NW device with 40 nm diameter exhibits a minimum S_{lin} of 70 mV/dec. The 20 nm diameter device shows a minimum S of 74 mV/dec at $V_{\text{DS}} = 0.5$ V. The D_{it} estimated from the linear subthreshold characteristics is approximately $3.9 \cdot 10^{12} \text{ eV}^{-1} \text{ cm}^{-2}$. Devices with such narrow diameters suffer from high contact resistance at low V_{DS} due to small top contact area. The inset of Fig. 3(c) shows that S remains below 80 mV/dec over two orders of magnitude of I_D . This is one of the best linear subthreshold swings reported in InGaAs VNW-MOSFETs, as shown in Fig. 4(d) [21]. This indicates that the new DE technique delivers sidewall quality comparable to the conventional approach.

V. CONCLUSIONS

In this work, a novel digital etch scheme utilizing alcohol-based etchants for use in III-V nanostructures is reported. The new approach exhibits excellent mechanical yield at sub-10 nm critical dimensions. Digital etch on the antimonide material system is demonstrated for the first time. Vertical nanowire InGaAs MOSFETs have been fabricated using the new technique. Subthreshold characteristics with minimum S of 70 mV/dec and 74 mV/dec are obtained on single NW MOSFET with diameters of 40 and 20 nm, respectively.

ACKNOWLEDGMENT

Device fabrication was carried out at the Microsystems Technology Laboratories and SEBL of MIT.

REFERENCES

- [1] K. J. Kanarik, T. Lill, E. A. Hudson, S. Sriraman, S. Tan, J. Marks, V. Vahedi, and R. A. Gottscho, "Overview of atomic layer etching in the semiconductor industry," *J. Vac. Sci. Technol. A*, vol. 33, no. 2, pp. 020802.1–020802.15, Mar. 2015, doi: 10.1116/1.4913379.
- [2] J. Yamamoto, T. Kawasaki, H. Sakaue, S. Shingubara, and Y. Horiike, "Digital etching study and fabrication of fine Si lines and dots," *Thin Solid Films*, vol. 225, no. 1, pp. 124–129, Mar. 1993, doi: 10.1016/0040-6090(93)90140-K.
- [3] G. C. DeSalvo, C. A. Bozada, J. L. Ebel, D. C. Look, J. P. Barrette, C. L. A. Cerny, R. W. Dettmer, J. K. Gillespie, C. K. Havasy, T. J. Jenkins, K. Nakano, C. I. Pettiford, T. K. Quach, J. S. Sewell, and G. D. Via, "Wet chemical digital etching of GaAs at room temperature," *J. Electrochem. Soc.*, vol. 143, no. 11, pp. 3652–3656, Nov. 1996, doi: 10.1149/1.1837266.
- [4] A. Alian, C. Merckling, G. Brammertz, M. Meuris, M. Heyns, and K. D. Meyer, "InGaAs MOS transistors fabricated through a digital-etch gate-recess process and the influence of forming gas anneal on their electrical behavior," *ECS J. Solid State Sci. Technol.*, vol. 1, no. 6, pp. 310–314, Jan. 2012, doi: 10.1149/2.001301jss.
- [5] S. Lee, C.-Y. Huang, D. Cohen-Elias, J. J. M. Law, V. Chobpattana, S. Krämer, B. J. Thibeault, W. Mitchell, S. Stemmer, A. C. Gossard, and M. J. W. Rodwell, "High performance raised source/drain InAs/In_{0.53}Ga_{0.47}As channel metal-oxide-semiconductor field-effect-transistors with reduced leakage using a vertical spacer," *Appl. Phys. Lett.*, vol. 103, no. 23, pp. 233503-1–233503-4, Dec. 2013, doi: 10.1063/1.4838660.
- [6] S. Lee, C.-Y. Huang, A. D. Carter, J. J. M. Law, D. C. Elias, V. Chobpattana, B. J. Thibeault, W. Mitchell, S. Stemmer, A. C. Gossard, and M. J. W. Rodwell, "High transconductance surface channel In_{0.53}Ga_{0.47}As MOSFETs using MBE source-drain regrowth and surface digital etching," in *Proc. Int. Conf. Indium Phosph. Rel. Mater. (IPRM)*, 2013, pp. 1–2, doi: 10.1109/ICIPRM.2013.6562630.
- [7] J. Lin, X. Zhao, D. A. Antoniadis, and J. A. del Alamo, "A novel digital etch technique for deeply scaled III-V MOSFETs," *IEEE Electron Device Lett.*, vol. 35, no. 4, pp. 440–442, Apr. 2014.
- [8] C. Y. Huang, P. Choudhary, S. Lee, S. Kraemer, V. Chobpattana, B. Thibeault, W. Mitchell, S. Stemmer, A. Gossard, and M. Rodwell, "12 nm-gate-length ultrathin-body InGaAs/InAs MOSFETs with $8.3 \cdot 10^5$ ION/IOFF," in *Proc. 73rd Annu. Device Res. Conf. (DRC)*, 2015, p. 260, doi: 10.1109/DRC.2015.7175669.
- [9] X. Zhao and J. A. del Alamo, "Nanometer-scale vertical-sidewall reactive ion etching of InGaAs for 3-D III-V MOSFETs," *IEEE Electron Device Lett.*, vol. 35, no. 5, pp. 521–523, May 2014.
- [10] X. Zhou, N. Waldron, G. Boccardi, F. Sebaai, C. Merckling, G. Eneman, S. Sioncke, L. Nyns, A. Opdebeek, J. W. Maes, Q. Xie, M. Givens, F. Tang, X. Jiang, W. Guo, B. Kunert, L. Teugels, K. Devriendt, A. S. Hernandez, J. Franco, D. van Dorp, K. Barla, N. Collaert, and A. V.-Y. Thean, "Scalability of InGaAs gate-all-around FET integrated on 300 mm Si platform: Demonstration of channel width down to 7 nm and Lg down to 36 nm," in *Proc. IEEE Symp. VLSI Technol.*, Honolulu, HI, USA, Jun. 2016, pp. 1–2, doi: 10.1109/VLSIT.2016.7573420.
- [11] A. J. A. Vardiand del Alamo, "Sub-10 nm fin-width self-aligned InGaAs-FinFETs," *IEEE Electron Devices Lett.*, vol. 37, no. 9, pp. 1104–1107, Sep. 2016, doi: 10.1109/LED.2016.2596764.
- [12] E. Memišević, J. Svensson, M. Hellenbrand, E. Lind, and L. E. Wernersson, "Scaling of vertical InAs-GaSb nanowire tunneling field-effect transistors on Si," *IEEE Electron Device Lett.*, vol. 37, no. 5, pp. 549–552, May 2016, doi: 10.1109/LED.2016.2545861.
- [13] N. Waldron, S. Sioncke, J. Franco, L. Nyns, A. Vais, X. Zhou, H. C. Lin, G. Boccardi, J. W. Maes, Q. Xie, M. Givens, F. Tang, X. Jiang, E. Chiu, A. Opdebeek, C. Merckling, F. Sebaai, D. van Dorp, L. Teugels, A. S. Hernandez, K. De Meyer, K. Barla, N. Collaert, and Y.-V. Thean, "Gate-all-around InGaAs nanowire FETS with peak transconductance of 2200uS/um at 50 nm Lg using a replacement fin RMG flow," in *IEDM Tech. Dig.*, Washington, DC, USA, Jul. 2015, pp. 31.1.1–31.1.4, doi: 10.1109/IEDM.2015.7409805.
- [14] X. Zhao, A. Vardi, and J. A. del Alamo, "InGaAs/InAs hetero-junction vertical nanowire tunnel FETs fabricated by a top-down approach," in *IEDM Tech. Dig.*, San Francisco, CA, USA, Dec. 2014, pp. 25.5-1–25-5.4, doi: 10.1109/IEDM.2014.7047108.
- [15] A. Vardi, X. Zhao, and J. A. del Alamo, "Quantum-size effects in sub 10-nm fin width InGaAs FinFETs," in *IEDM Tech. Dig.*, Washington, DC, USA, Dec. 2015, pp. 31.3-1–31-3.4, doi: 10.1109/IEDM.2015.7409807.
- [16] A. Nainani, T. Irisawa, Z. Yuan, Y. Sun, T. Krishnamohan, M. Reason, B. R. Bennett, J. B. Boos, M. G. Ancona, Y. Nishi, and K. C. Saraswat, "Development of high-k dielectric for antimonides and a sub 350 C III-V pMOSFET outperforming germanium," in *IEDM Tech. Dig.*, San Francisco, CA, USA, Dec. 2010, pp. 6.4-1–6-4.4, doi: 10.1109/IEDM.2010.5703309.
- [17] W. Lu, J. K. Kim, J. F. Klem, S. D. Hawkins, and J. A. del Alamo, "An InGaSb p-channel FinFET," in *IEDM Tech. Dig.*, Washington, DC, USA, Dec. 2015, pp. 31.6-1–31-6.4, doi: 10.1109/IEDM.2015.7409810.
- [18] Q. Smets, A. S. Verhulst, S. El Kazzi, D. Gundlach, C. A. Richter, A. Mocuta, N. Collaert, A. V.-Y. Thean, and M. M. Heyns, "Calibration of the effective tunneling bandgap in GaAsSb/InGaAs for improved TFET performance prediction," *IEEE Trans. Electron Devices*, vol. 63, no. 11, pp. 4248–4254, Nov. 2016, doi: 10.1109/TED.2016.2604860.
- [19] C. Thelander *et al.*, "Development of a vertical wrap-gated InAs FET," *IEEE Trans. Electron Devices*, vol. 55, no. 11, pp. 3030–3036, Nov. 2008.
- [20] X. Zhao, J. Lin, C. Heidelberger, E. A. Fitzgerald, and J. A. del Alamo, "Vertical nanowire InGaAs MOSFETs fabricated by a top-down approach," in *IEDM Tech. Dig.*, Dec. 2013, pp. 28.4.1–28.4.4, doi: 10.1109/IEDM.2013.6724710.
- [21] J. A. del Alamo, D. A. Antoniadis, J. Lin, W. Lu, A. Vardi, and X. Zhao, "Nanometer-scale III-V MOSFETs," *IEEE J. Electron Device Soc.*, vol. 4, no. 5, pp. 205–214, Sep. 2016, doi: 10.1109/JEDS.2016.2571666.